

UC Irvine

UC Irvine Previously Published Works

Title

Multicolor fluctuation spectroscopy in cells

Permalink

<https://escholarship.org/uc/item/5b02k7d4>

Authors

Digman, Michelle A
Gratton, Enrico

Publication Date

2009-02-12

DOI

10.1117/12.814875

Copyright Information

This work is made available under the terms of a Creative Commons Attribution License, available at <https://creativecommons.org/licenses/by/4.0/>

Peer reviewed

Multicolor fluctuation spectroscopy in cells

Michelle A. Digman^{a,b} and Enrico Gratton^a

^aLaboratory for Fluorescence Dynamics, Dept. of Biomedical Engineering, ^bOptical Biology Core, Development Biology Center, University of California, Irvine, CA 92697, USA

ABSTRACT

Based on the Fluctuation Correlation principle we have developed a method that is capable of measuring the stoichiometry of molecular complexes and mapping dynamic processes in living cells. The method is based on measuring simultaneously fluctuations of the fluorescence intensity at two image channels, each detecting a different kind of protein. This is an extension of the number and brightness analysis in which we use the use of the ratio between the variance and the average intensity to obtain the brightness of molecules.

Keywords: Fluorescence microscopy, Fluctuation spectroscopy, Brightness analysis, Protein complexes, Focal adhesion

1. INTRODUCTION

Fluorescence correlation spectroscopy (FCS) is a method based on spontaneous fluctuations used to measure reactions and diffusion in solutions and in cells at the single molecule level. FCS was first applied to biological materials about 30 years ago by the pioneering work of Elson et al¹. As originally conceived, the FCS technique measures the intensity fluorescence fluctuations in a single position in the sample. The autocorrelation of the intensity fluctuations is then calculated and the kinetic parameters of the physical or chemical process that generate the fluctuations are obtained²⁻⁴. When we first applied FCS to the interior of the cells, a series of problem arose⁵. The average intensity suddenly changed, perhaps due to the passage of a large vesicle at the point of observation. Bleaching of the immobile fraction occurred, causing a large deviation of the apparent correlation curve. The cell could have moved, so that the volume of observation was not any more the chosen one.

Manufacturers such as Zeiss and ISS that have built FCS instrument for solution experiments were confronted with the request by many researchers to be able to directly perform FCS measurements in cells. Zeiss came out with the Confocor 2 and now Confocor 3 instruments, in which it was possible to alternate the capability of performing FCS at one point with the confocal unit. ISS produced an instrument in which it was possible to raster scan the sample in a “conventional FCS unit”, thereby joining imaging with FCS, but always at two separate times. We took a radically different approach in which we rapidly measured the intensity fluctuations in many points in the sample quasi-simultaneously introducing the scanning FCS principle.⁵

1.1 Scanning FCS

If we could move the point at which we acquire FCS data fast enough to other points in the sample and then return to the original point “before” the particle had left the volume of excitation, then we can “multiplex the time” and collect FCS data at several points simultaneously (Figure 1)

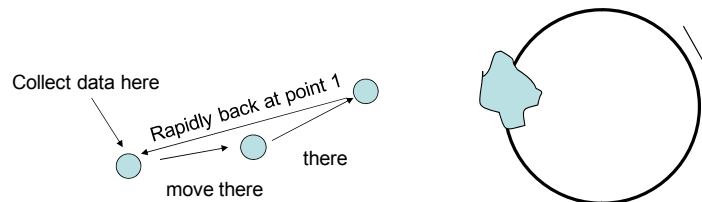


Fig. 1. Data are collected moving the scanner rapidly to different points so that particles don't have enough time to move out of the observation volume during a line or orbit scan.

The fastest way to scan several points and then return to the original point is to perform a circular orbit using the scanner galvo. The x- and y-galvos are driven by 2 sine waves shifted by 90 degrees, thereby obtaining a projected orbit on the sample. One orbit could be performed in times of less than 1 ms using conventional galvo drivers and in microseconds using acousto-optic deflectors. However, in most commercial instruments, the circular scanning capability is not offered. Although less efficient and slower, the same effect, namely measure one point and return to the same point before the molecule has moved away, can be obtained with line-scanning.

The minimum time required for an orbit or a line scan that will not miss the “fastest” diffusion process in a cell is determined by the average time a molecule takes to diffuse across the excitation beam waist, which is on the order of $0.35\mu\text{m}$ in our microscope (Figure 2)

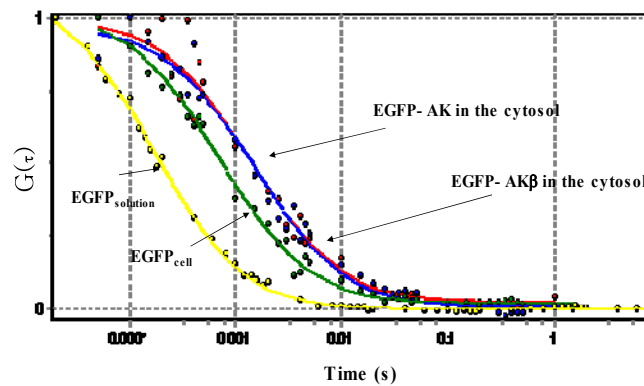


Fig. 2. Diffusion times of typical molecules in solution and in cells. For EGFP in cells, the characteristic diffusion time is in the ms range. For larger proteins such as EGFP-AKb in the cytosol, the diffusion time is slower.

In cells, EGFP diffuses with an apparent diffusion coefficient of approximately $D=20\mu\text{m}^2/\text{s}$. Transit across the laser beam waist (assuming a waist w_0 of $0.35\mu\text{m}$) occurs in about 1.5 ms ($time = \frac{w_0^2}{4D}$). Therefore 0.5 to 1 ms per orbit or line should catch the EGFP molecule diffusing in a cell at the next orbit and at the same location before the molecule leaves the volume of excitation. Instead faster diffusing molecules will be partially missed.

1.2 Acquiring scanning-FCS data

Light is collected along the orbit, generally at 64 or 128 points. If the orbit period is 1ms, the dwell time at each point is about $16\mu\text{s}$ (64 points) or $8\mu\text{s}$ (128 points). The separation between the points depends on the orbit radius. For an orbit radius of $5\mu\text{m}$, the length of the orbit is about $32\mu\text{m}$. At 64 points per orbit the average distance is about $0.5\mu\text{m}$ ($0.25\mu\text{m}$ at 128 points). Why the distance between points is important?

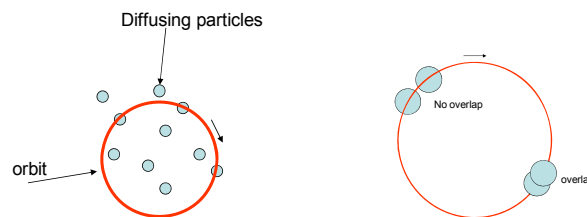


Fig. 3. Overlapping volumes in scanning FCS. Points along the scan line must be close enough so that the same particle is oversampled.

1.3 Overlapping volumes in scanning FCS

If the orbit is larger than $5\ \mu\text{m}$, the points are separated by more than the width of the PSF. Setting the conditions of the instrument for no-overlap limits the capability of obtaining spatial correlations along the orbit, as will be explained later (Figure 3). If we use overlapping excitation volumes, even if the molecule diffuses very fast, the same molecule can be seen in the adjacent pixels along the orbit. This is the basis for the RICS method (raster scan image correlation spectroscopy) previously described⁶.

2. CARPET ANALYSIS

In the following we show how from the data collected along the orbit we can determine the diffusion of particles, the number of particles and their brightness. Recently, others approaches have been used to obtain the diffusion parameters from scanning FCS⁷ in which the scanning motion and the sampling of points along the orbit is not synchronized.

2.1 Data presentation and processing in scanning FCS

In this section we show simulated data for a system of 20 particles freely diffusing in a square region of $12.5\ \mu\text{m}$ side with a diffusion coefficient of $0.1\ \mu\text{m}^2/\text{s}$. Data are collected along a circle as shown in figure 4 sampling 64 points along the orbit.

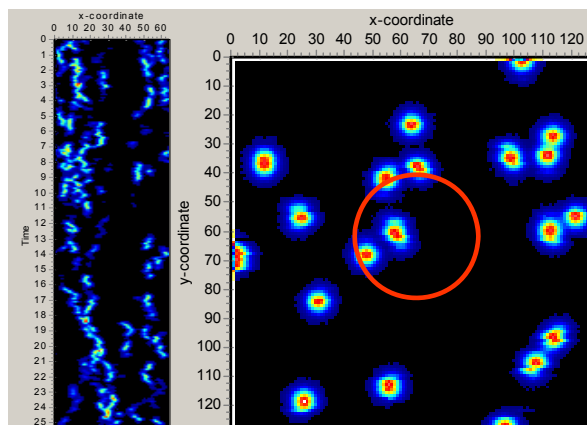


Fig. 4. Left panel: Carpet representation of the data collected along the scan line or orbit. Right panel: snapshot image of the particles in the field of view and placement of the orbit.

If we select a column of the carpet, it is a time sequence at a specific point of the orbit or line scan. We can then perform the autocorrelation operation on this time sequence and obtain the correlation function at a specific location in the cell. The sampling time at this location is given by the scan time, not the pixel time. The fit of the autocorrelation curve using the equations for diffusion given in the Material and Method section provide the value of the diffusion coefficient and the $G(0)$, from which we can calculate the number of particles in the volume of excitation. The particle brightness can be directly obtained using the Number and Brightness analysis (N&B) at each column^{8,9}.

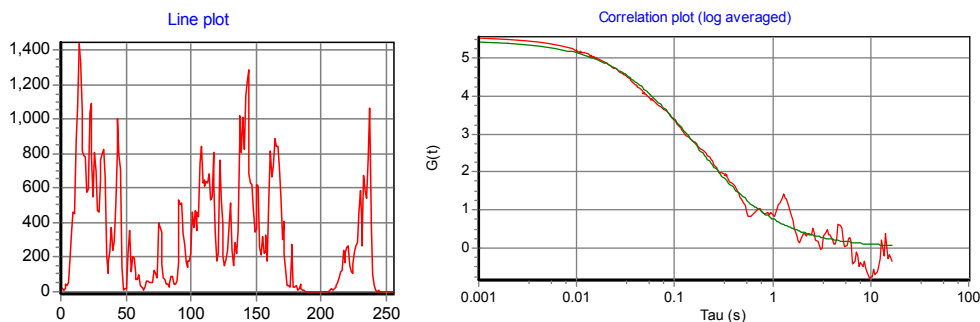


Fig. 5. Left plot: intensity along a column. For this figure 100 orbits were averaged for each data point. Right panel: averaged autocorrelation function calculated using the time sequence at each individual column of the carpet.

Every column should be equivalent for a homogeneous sample, so that we can calculate the autocorrelation function for every column and then fit all the columns either globally or individually.

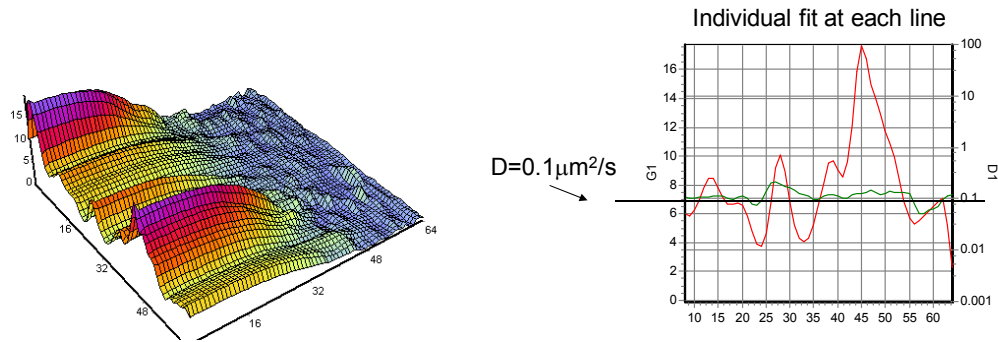


Fig. 6. Left panel: 3D representation of the autocorrelation of the carpet. Right panel: Fit of the autocorrelation function using a 2D diffusion model. Red is G_0 and green is the recovered diffusion coefficient.

2.2 Example of scanning at an adhesion

In this section we show data collected in a biological samples consisting of a culture of MEF cells (mouse embryonic fibroblast, see Material and Method section) co-expressing the protein FAK-EGFP (focal adhesion kinase) and paxillin-mCherry. Both proteins are constituent of focal adhesions. First we show that in the “real world” there are strong intensity changes due to the bleaching of the proteins that are bound to the adhesions.

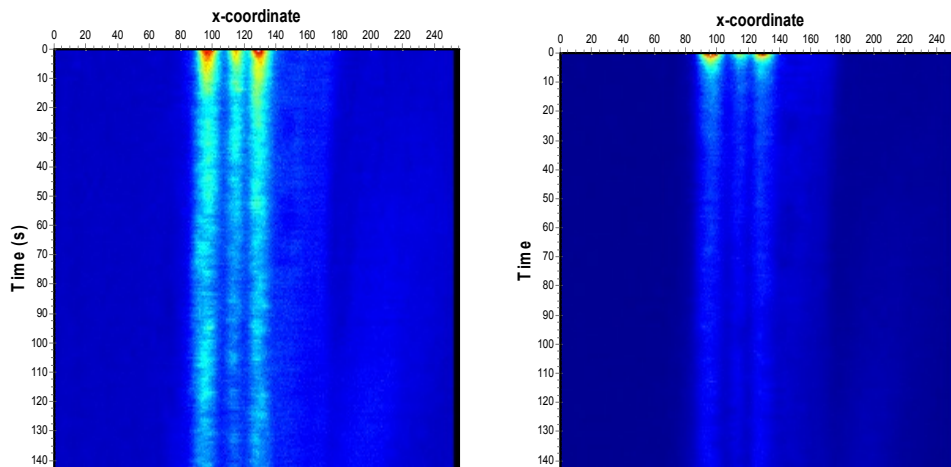


Fig. 7. Left panel is the carpet for the “green” channel (EGFP) and right panel; is the carpet for the red channel (mCherry). Data are collected using a scan line of 4.35 ms in the Olympus FV1000 laser confocal microscope 256 points are collected along a line scan. The distance between points in the scan is 50 nm. At the beginning of the time sequence there is a strong decrease of the fluorescence intensity due to bleaching.

Before we can do any analysis of the intensity fluctuations, we must account for the very large “intensity fluctuations” due to bleaching. This change of intensity is correlated in both acquisition channels and without proper treatment it will give the appearance of correlated fluctuations in both channels.

Figure 7 shows that in the initial 10 s there is substantial bleaching of the sample as shown by the large decrease of intensity. The specific scan line used is shown in figure 8.

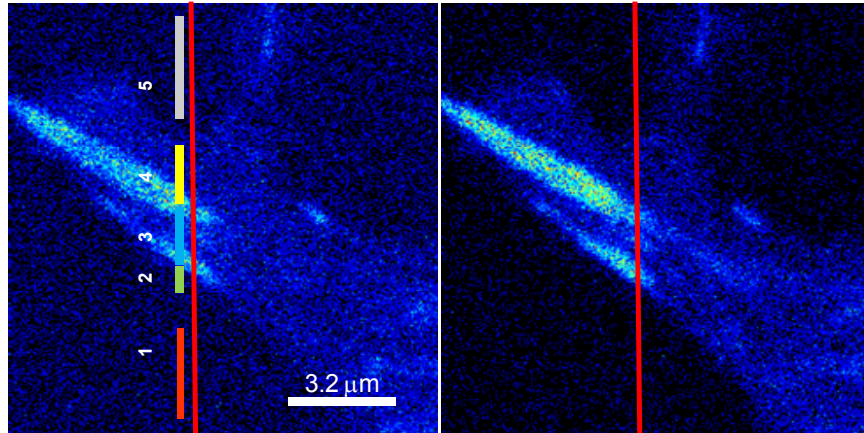


Fig. 8. Detail of the MEF cell and of the position of the scan line. Data obtained with the Olympus FV100 laser confocal microscope. The two panels left and right correspond to the green and the red channels of the microscope, respectively.

Figure 8 shows a detail of an image of a cell expressing FAK-EGFP and Paxillin-mCherry. Data are collected in different parts of the cell, including the exterior (to be used for control), across 3 adhesions and in a region where adhesions are disassembling.

The red line indicates the line of scanning. Each line is scanned in 4.35 ms and the line contains 256 points. The pixel distance along the line is 50 nm. For each experiment 32k lines were acquired for a total time of about 142s. The data are presented as a carpet where the horizontal coordinate corresponds to points along the orbit and the vertical coordinate correspond to different times.

Data were corrected for this initial trend using a high pass filter that filters out all the time changes with periods longer than approximately 10 s and the first and last 10 s were disregarded from the analysis (Figure 9).

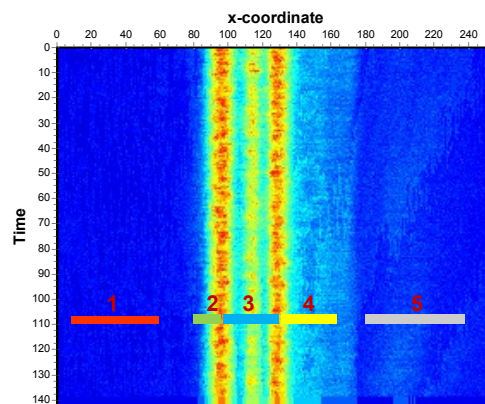


Fig. 9. Carpet after correction for changes in intensity due to bleaching. The regions 1 to 5 indicated in the figure correspond to parts of the image with different cell features. Region 1 is outside the cell. Region 2-4 the line scan is over adhesions and 5 corresponds to a region where the adhesions are mainly disassembling.

3. STOICHIOMETRY OF PROTEIN COMPLEXES

In this section we show how to analyze data collated in the line scan mode in two channels simultaneously to extract the parameters for the formation and stoichiometry of complexes in live cells. Among the many biological questions, here we focus in a) determine if the FAK and paxillin proteins are diffusing in the cytoplasm of the MEF cells, b) if the two

proteins (which are known to be interacting partners) are complexed in the cytoplasm and then jointly assembled at the adhesion or rather they bind to the adhesion independently, c) the stoichiometry of the protein complex.

3.1 Autocorrelation and cross-correlation

First we calculate the autocorrelation function in the two channels and the amount of cross-correlation¹⁰⁻¹³.

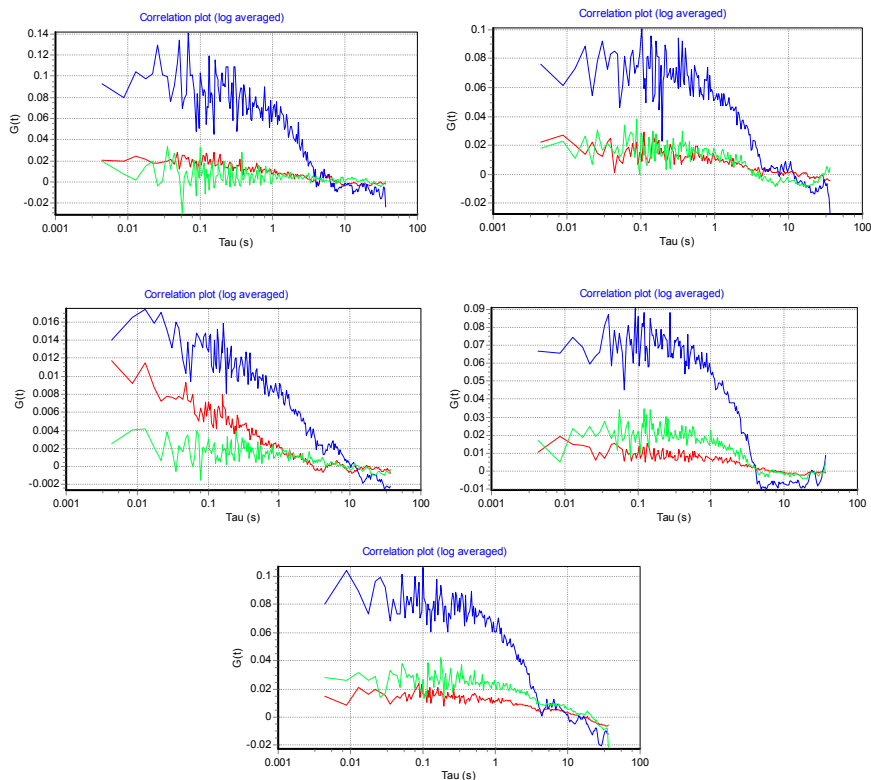


Fig. 10. Autocorrelation of channel 1(red) channel 2(blue) and cross-correlation (green) in the 5 regions indicated in figure 9, in order, respectively.

To evaluate the amount of cross-correlation in the various regions analyzed we calculated the ratio $G_{cc}(0)/AVG(G1(0),G2(0))$, where G_{cc} is the cross-correlation amplitude and $G1(0)$ and $G2(0)$ are the amplitude of the autocorrelation for channel 1 and 2, respectively. In the graph below we show that the amount of cross correlation is maximal in the region at the borders of the disassembling adhesion, in agreement with previous reports¹⁴.

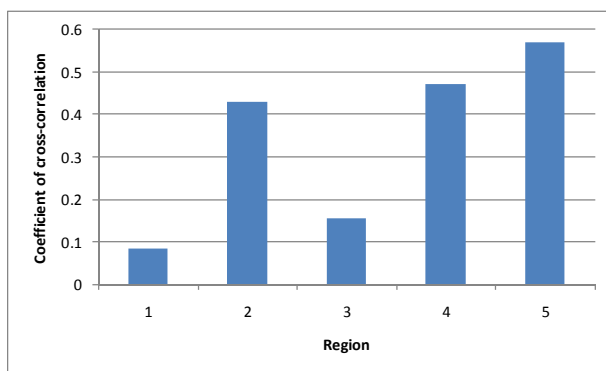


Fig. 11. Coefficient of cross-correlation $G_{cc}(0)/AVG(G1(0),G2(0))$, in the 5 different regions shown in figure 9. The cross-correlation is maximal at the borders of the adhesions and in the region of disassembling adhesions.

However, using the line scanning method we have substantially improved the spatial resolution from about $2\ \mu\text{m}$ to about $0.2\ \mu\text{m}$) and we can confidently assign the interaction of the two proteins studied to specific regions of the adhesion.

From the time correlation analysis at each point along the line scan we conclude that only at the adhesions and in specific regions of the cell interior are the two proteins, FAK and paxillin, interacting. However, the cross-correlation analysis is not giving information about the size and the stoichiometry of the complex, i.e., how many molecule of FAK and of paxillin are part of the complex that shows cross-correlation.

3.2 Brightness and cross-brightness analysis.

In Figure 12 we show the analysis of the brightness for channel 1 (red) and channel 2 (blue) and the analysis of the cross-variance (green) (See Material and Methods section for the equations used to define brightness and cross-brightness) . In accord with the cross-correlation analysis, only in the regions 2, 4 and 5 there is substantial positive cross-variance. Note also that the brightness of the two channels is relatively high in these regions. However, the plot of the cross-variance as a function of the position along the orbit is not telling us if the fluctuations that have large variance are occurring at the same time.

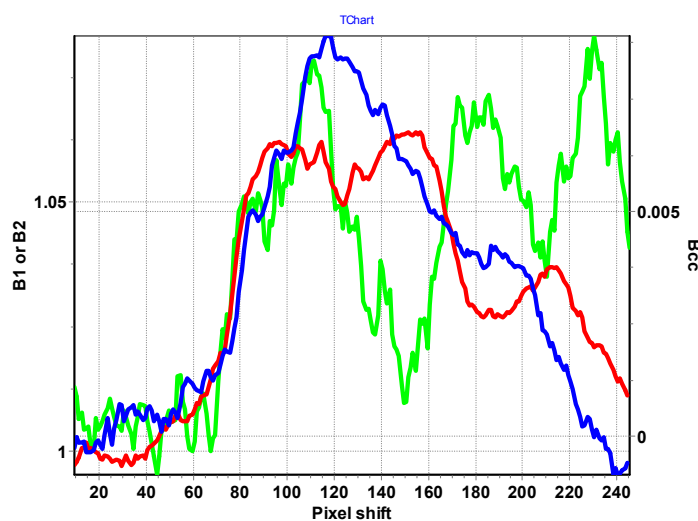


Fig. 12. Brightness and cross-brightness analysis along the line scan. The red line is for B1 (FAK-EGFP), the blue line for B2 (paxillin-mCherry) and the green line is the cross-brightness Bcc (right vertical axis).

To establish the size of the fluctuations in both channels simultaneously and in coincidence with the occurrence of large cross-variance, we scan the time sequence at any given pixel along the scan line so that when we get a positive cross-variance above a given threshold we record the B values of both channels for that fluctuation. If we normalize the B values of both channels to the value of the brightness of the monomer, we could calculate the brightness of the particle in both channels that has a cross-correlated fluctuation.

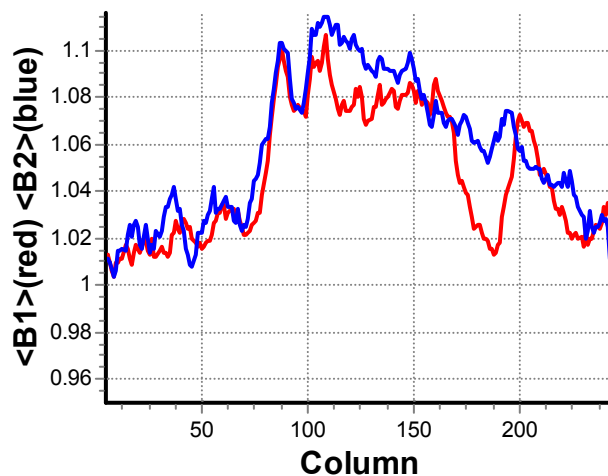


Fig. 13. Cross-brightness analysis along the line scan. The red line is for Channel 1 (FAK-EGFP) and the blue line for Channel 2 (paxillin-mCherry). The threshold for the cross-variance was set to 0.01 and the entire time sequence (140 s) at each point along the line was divided in 50 segments of about 2.8 s each.

Independent determinations for the brightness of the monomers in channel 1 and 2 were 1.02 and 1.025, respectively. On this basis we estimate that at the adhesions, the complexes are composed of approximately 5 units of each protein.

4. CONCLUSIONS

Even in the “simplest” implementation, FCS in cells requires precautions in data analysis and interpretation. Maps of diffusion coefficients, number of particles and brightness can be obtained if we can deal with slowly varying fluctuations. The software for data analysis must offer a series of tools to the user for data filtering, analysis and presentation. It is not enough to collect line scanning data. The user must set up the instrument parameters (line period, dwell time, etc) for the particular experiment. The line scan analysis provides a very robust approach for detrending the data for bleaching effects or other slow changing signals that strongly perturb the shape of the autocorrelation function. The brightness and the cross-brightness analysis can be done at each point along the line scan providing a method to evaluate the brightness of the particles that fluctuate simultaneously in both channels. From these correlated fluctuations in time and amplitude, we determined the average stoichiometry of the complexes.

5. MATERIALS AND METHODS

Sample preparation and microscope setup was previously described and is repeated here for the reader convenience¹⁵.

Cell culture and protein transfection. Mouse Embryonic Fibroblasts (MEF) were grown at 37°C in a 5% CO₂ humidified incubator. The cells were trypsinized, subcultured and transferred from a 35mm tissue culture flask to a 25mm, 6 well Falcon tissue culture (Becton-Dickinson, Bedford, MA). They were grown to 50-80% confluency and transfected with 1 μg of DNA (0.5μg of DNA/protein for co-transfections) and 5μg of lipofectamine 2000 obtained from Invitrogen (Carlsbad, CA). FAK (Focal Adhesion Kinase) and paxillin cDNA were ligated to EGFP or mCherry at the C-terminal end¹⁶. After 24 h of transfection cells were trypsinized and plated using High Glucose DMEM media (Pierce-Hyclone, Logan, UT) supplemented with 10% FBS and PEN/STREP on MatTek (Ashland, MA) imaging dishes coated with 3 μg of fibronectin from Sigma-Aldrich (Louis, MO) one hour prior to imaging.

Microscopy. We used an Olympus FV1000 microscope with a 60x 1.2NA water objective (Olympus, Tokyo, Japan). The scan speed was set at 12.5 us/pixel. The scan area was 256x256 pixels. The corresponding line time was 4.325 ms. The electronic zoom of the microscope was set to 16.3, which corresponds to a line length of 20.5 μm. For the EGFP excitation, we used the 488nm line of the argon ion laser and for the mCherry excitation we used the 559nm line from a

HeNe laser. The power of the 488nm laser was set at 0.5% according to the power slider in the FV1000 microscope. The power of the red laser was then changed to match the average intensity in the two channels. Generally, the power in the red channel was below 1.5%. Data were collected in the pseudo photon counting mode of the Olympus FV1000 microscope. The filters for the green and red emission channels have a nominal bandwidth of 505-540nm and 575-675 nm, respectively. The overlap of the volume of observation and excitation at the two colors of our experiments was tested by imaging single 100 nm fluorescent beads carrying two colors simultaneously (Yellow-green fluorospheres, Invitrogen, Carlsbad, CA). We imaged single immobilized beads using a z-stack with images acquired every 500nm in the z direction. We found that in the FV1000 microscope the center of mass of the excitation volumes were coincident within 20 nm in the x and y direction and within about 40 nm in the z direction in both channels

Data analysis. We used the SimFCS program (Laboratory for Fluorescence Dynamics) for the autocorrelation, cross-correlation and N&B analysis along the scan-line. Fitting of the correlation functions for the simulated data was performed according to the equations for diffusion.

$$G(\tau) = \frac{\gamma}{N} \left(1 + \frac{4D\tau}{w_{3DG}^2} \right)^{-1} \left(1 + \frac{4D\tau}{z_{3DG}^2} \right)^{-1/2} \quad (1)$$

Where the factor γ depends on the volume of excitation, N is the average number of molecules in the volume of excitation, D is the diffusion coefficient and w indicates the beam waist assumed to be Gaussian in the radial and z dimensions, respectively.

One of the features of the scanning FCS data analysis is that slowly varying signals (fluctuations) can be removed from the calculation using a high-pass filter operation implemented by a moving average operation. The moving average processing of the data stack removes the correlations due to the slowly changing signal. The length of the moving average determines the time scale of processes that are filtered out by this mathematical procedure.

For the brightness analysis the equations used are the following

$$\langle k \rangle = \frac{\sum_i k_i}{K} \quad (2)$$

$$\sigma^2 = \frac{\sum_i (k_i - \langle k \rangle)^2}{K} \quad (3)$$

Where k_i is the fluorescence intensity at the position i along the line scan and K is the total number of line scans, generally 32k. These are just the definitions of average intensity and variance at a point along the line scan. The brightness B and the number N are defined according to the following relationships

$$B = \frac{\langle k \rangle}{\langle N \rangle} = \frac{\sigma^2}{\langle k \rangle} \quad (4)$$

$$\langle N \rangle = \frac{\langle k \rangle^2}{\sigma^2} \quad (5)$$

The cross variance is defined as

$$\sigma_{cc}^2 = \frac{\sum (G_i - \langle G \rangle)(R_i - \langle R \rangle)}{K} \quad (6)$$

where G_i and $\langle G \rangle$ refer to the intensity at a point and the average along a column of green channel and R_i and $\langle R \rangle$ refers to the red channel. The Bcc term is defined as

$$B_{cc} = \frac{\sigma_{cc}^2}{\sqrt{\langle G \rangle \langle R \rangle}} \quad (7)$$

Acknowledgements: Work supported in part by U54 GM064346 Cell Migration Consortium (MD and EG), NIH-P41 P41-RRO3155 (EG) and P50-GM076516 (EG). We thank Dr. Paul Wiseman for his work done at the Laboratory for Fluorescence Dynamics during the period September 2007-March 2008 and for collecting the line scan data used for this paper.

References

1. Elson, E.L. & Webb, W.W. Concentration correlation spectroscopy: a new biophysical probe based on occupation number fluctuations. *Annu Rev Biophys Bioeng* **4**, 311-334 (1975).
2. Elson, E.L. Fluorescence photobleaching and correlation spectroscopy for translational diffusion in biological systems. *Biochem Soc Trans* **14**, 839-841 (1986).
3. Elson, E.L. Fluorescence correlation spectroscopy measures molecular transport in cells. *Traffic* **2**, 789-796 (2001).
4. Schwille, P., Bieschke, J. & Oehlenschläger, F. Kinetic investigations by fluorescence correlation spectroscopy: the analytical and diagnostic potential of diffusion studies. *Biophys Chem* **66**, 211-228 (1997).
5. Berland, K.M., So, P.T. & Gratton, E. Two-photon fluorescence correlation spectroscopy: method and application to the intracellular environment. *Biophys J* **68**, 694-701 (1995).
6. Digman, M.A. et al. Measuring fast dynamics in solutions and cells with a laser scanning microscope. *Biophys J* **89**, 1317-1327 (2005).
7. Ries, J. & Schwille, P. Studying slow membrane dynamics with continuous wave scanning fluorescence correlation spectroscopy. *Biophys J* **91**, 1915-1924 (2006).
8. Digman, M.A., Dalal, R., Horwitz, A.F. & Gratton, E. Mapping the number of molecules and brightness in the laser scanning microscope. *Biophys J* **94**, 2320-2332 (2008).
9. Dalal, R.B., Digman, M.A., Horwitz, A.F., Vetri, V. & Gratton, E. Determination of particle number and brightness using a laser scanning confocal microscope operating in the analog mode. *Microsc Res Tech* **71**, 69-81 (2008).
10. Schwille, P., Meyer-Almes, F.J. & Rigler, R. Dual-color fluorescence cross-correlation spectroscopy for multicomponent diffusional analysis in solution. *Biophys J* **72**, 1878-1886 (1997).
11. Bacia, K. & Schwille, P. Practical guidelines for dual-color fluorescence cross-correlation spectroscopy. *Nat Protoc* **2**, 2842-2856 (2007).
12. Hausteiner, E. & Schwille, P. Fluorescence correlation spectroscopy: novel variations of an established technique. *Annu Rev Biophys Biomol Struct* **36**, 151-169 (2007).
13. Bacia, K., Kim, S.A. & Schwille, P. Fluorescence cross-correlation spectroscopy in living cells. *Nat Methods* **3**, 83-89 (2006).
14. Digman, M.A., Brown, C.M., Horwitz, A.R., Mantulin, W.W. & Gratton, E. Paxillin dynamics measured during adhesion assembly and disassembly by correlation spectroscopy. *Biophys J* **94**, 2819-2831 (2008).
15. Digman, M.A., Paul Wiseman, Alan R. Horwitz, and Enrico Gratton. Detecting protein complexes in living cells from laser scanning confocal image sequences by the ccRICS method *Biophysical Journal* (in press) (2009).
16. Choi, C.K. et al. Actin and alpha-actinin orchestrate the assembly and maturation of nascent adhesions in a myosin II motor-independent manner. *Nat Cell Biol* **10**, 1039 - 1050 (2008).